Solution Structure of Copper Ion-Induced Molecular Aggregates of Tyrosine Melanin

J. M. Gallas,* K. C. Littrell,# S. Seifert,§ G. W. Zajac,¶ and P. Thiyagarajan#

*Division of Earth and Physical Sciences, University of Texas at San Antonio, San Antonio, Texas 78249; #Intense Pulsed Neutron Source and §Chemistry Division, Argonne National Laboratory, Argonne, Illinois 60439; and ¶Amoco Research Center, Naperville, Illinois 60566-7011 USA

ABSTRACT Melanin, the ubiquitous biological pigment, provides photoprotection by efficient filtration of light and also by its antioxidant behavior. In solutions of synthetic melanin, both optical and antioxidant behavior are affected by the aggregation states of melanin. We have utilized small-angle x-ray and neutron scattering to determine the molecular dimensions of synthetic tyrosine melanin in its unaggregated state in D_2O and H_2O to study the structure of melanin aggregates formed in the presence of copper ions at various copper-to-melanin molar ratios. In the absence of copper ions, or at low copper ion concentrations, tyrosine melanin is present in solution as a sheet-like particle with a mean thickness of 12.5 Å and a lateral extent of ~54 Å. At a copper-to-melanin molar ratio of 0.6, melanin aggregates to form long, rod-like structures with a radius of 32 Å. At a higher copper ion concentration, with a copper-to-melanin ratio of 1.0, these rod-like structures further aggregate, forming sheet-like structures with a mean thickness of 51 Å. A change in the charge of the ionizable groups induced by the addition of copper ions is proposed to account for part of the aggregation. The data also support a model for the copper-induced aggregation of melanin driven by π stacking assisted by peripheral Cu^{2+} complexation. The relationship between our results and a previous hypothesis for reduced cellular damage from bound-to-melanin redox metal ions is also discussed.

INTRODUCTION

Melanin is a ubiquitous pigment responsible for much of the coloration in nature. In animals and humans it is found in the hair, skin, and eyes, where its principal function is considered to be that of photoprotection (Kollias, 1995; Pathak and Fitzpatrick, 1974; Young, 1998). It is also found in the mid-brain and in the inner ear (Ishii, 1984). Much attention has, therefore, been given to the far-reaching functionality and properties of melanins. We believe that this multifunctionality should be reflected in a highly evolved, unique melanin structure. However, neither the size nor the structure of the fundamental molecular unit of the melanins has been well-understood as yet.

Our interest is in looking at the smallest molecular units that may be considered to have the properties of melanin and from which aggregation in solution occurs. Previous wide-angle x-ray scattering (WAXS) experiments have led to models for a "local structure" for melanin (Cheng et al., 1994) wherein five to seven 5,6-indolequinone units are arranged in planes which are π-stacked with a spacing of ~3.4 Å (Chio, 1977). This 3.4 Å spacing corresponds to the most prominent diffraction peak in the WAXS data. A less prominent peak in the WAXS data of powder samples of some melanins suggested that an additional repeat distance of ~15 Å exists. In subsequent studies, scanning tunneling microscopy (STM) was used to image the same tyrosine melanin precipitated from highly dispersed, dilute solutions onto highly oriented pyrolytic graphite substrates from solutions of tetrahydrofuran (THF) (Zajac et al., 1994). In that work a typical STM image was presented alongside the model for the local structure used to fit previous wide-angle x-ray diffraction data for tyrosine-derived melanin (Zajac et al., 1994). The typical melanin structures observed by STM are 15–20 Å in lateral extent and ~10 Å in height. The compact three-dimensional structure observed in the STM image is compatible with the model of stacked layers of 5,6-indolequinone that was used to analyze the WAXS data. By providing direct imaging of dispersed melanin, the recent STM analysis supports the view that the 15 Å repeat distance seen in the WAXS data of powder samples of some melanins may correspond to the size of the fundamental melanin molecule, which we also refer to as the melanin "protomolecule."

The objective of the present study is to elucidate the structure of the protomolecule in the aqueous phase and to understand the mechanism of aggregation in the presence of copper ions. One impediment to probing the structure of the fundamental melanin molecule is the apparent tendency for it to readily aggregate in samples prepared under different conditions (Eisner, 1992; Kozikowski et al., 1984). Earlier SAXS studies (Miyake et al., 1986) of melanin derived from various precursors in aqueous solutions indicated that the aggregates have R_g (radius of gyration) values between ~15 Å and ~50 Å with shapes ranging from spheres to rods. The size and structure of melanin aggregates produced by systematic changes in the pH of aqueous melanin solutions have been studied by using static and dynamic light scat-

Received for publication 4 December 1998 and in final form 19 May 1999.

Address reprint requests to Dr. J. M. Gallas, Division of Earth and Physical Sciences, University of Texas at San Antonio, 6900 N. Loop 1604 West, San Antonio, TX 78249-0663. Tel.: 210-458-5446; Fax: 210-458-4469; E-mail: jgallas@lonestar.utsa.edu.

0006-3495/99/08/1135/08 $2.00

tering. The resulting aggregates, which range in size from ~200 Å to microns, were shown to form mass fractals with dimensions ranging from 1.8 in the reaction-limited regime to 2.2 in the diffusion-limited regime (Huang et al., 1989). More recently, light-scattering techniques were used to characterize both the molecular weights and radii of gyration for natural and synthetic melanins during the polymerization and aggregation stages (Bridelli, 1998).

The tendency for melanin to aggregate may have caused investigators to associate micron sizes with the molecular structures of melanin based on the data from melanin samples in their aggregated states (Zeise, 1995). The natural tendency of melanin to aggregate under a variety of conditions of physiological relevance suggests that the structural changes associated with aggregation may relate to its function (Chedekel, 1995). For example, aggregates of synthetic melanins have redox reaction rates different from those for unaggregated melanins, suggesting that these reaction rates may be related to size and structure of the melanin aggregates (Sarna, 1992). Due to the potential influence of the aggregation of melanin on its function as a photoprotective agent, it is important to characterize and understand the systematic structural evolution of the melanin aggregate from its fundamental state in highly dispersed solutions.

To our knowledge there have been no structural studies on metal ion-induced aggregation of melanins, nor any attempts to characterize the structural bridge between the melanin protomolecule and its much larger aggregates. The primary purpose of this paper is to characterize the size and morphology of synthetic tyrosine melanin from its unaggregated or nearly unaggregated initial state through the early stages of its metal ion-induced aggregation. At low molar copper ion concentrations we expect an early stage of aggregation, which should be characterized by the association of small numbers of melanin protomolecules. In the present study we use small-angle neutron scattering (SANS) and small-angle x-ray scattering (SAXS), using synchrotron x-rays, to investigate the size and morphology of particles of tyrosine melanin in aqueous solutions at several copper ion concentrations. We believe that the current study, using SANS and SAXS on synthetic melanins in aqueous media, could provide a basis on which to approach the modeling of natural melanin aggregation. If aqueous melanin solutions consist of unaggregated protomolecules, then they will have particles with R_g values ~7 Å (See Note 1 at end of text). This size will be at the borderline limit of SANS detection, but SAXS at the high flux synchrotron sources will provide the high-quality data necessary to study these systems.

EXPERIMENTAL

Melanin preparation

To choose the appropriate solvent that provides a large contrast for neutron scattering we calculated the scattering length density of the components using the expression

$$\rho = (dN_A/M_w)\sum_i b_i, \quad (1)$$

where b_i is the neutron scattering length of the ith atom in the fundamental molecule, N_A is Avogadro's number, and M_w and d are the mass and the mass density of the molecules or their aggregates in solution, respectively.

The neutron scattering length densities of H_2O and D_2O are -0.56×10^{10} cm^{-2} and 6.34×10^{10} cm^{-2}, respectively. The scattering length density of a melanin monomer is 3.57×10^{10} cm^{-2}, based on the chemical formula $C_{48}O_{12}N_6H_{20}$ for the 5,6-indolequinone used in the WAXS model and a measured density of 1.4 g/cm^3 for melanin in solution (see Note 2). Since the SANS signal scales as the square of the difference in the scattering length densities of melanin and the solvent, it is clear that the coherent scattering signals will be stronger if measured in H_2O. The actual contrast for SANS of melanin dispersed in D_2O will be lower than that expected from the calculated difference in their scattering length densities due to the exchange of protons from the sample with the deuterons in the solvent. Hence, most of the SANS experiments were conducted in H_2O, although a few were done in D_2O.

Aqueous solutions of synthetic melanin at a concentration of 1 g/10 cm^3 of water were prepared using tyrosine-derived melanin purchased from Genzyme Corporation (Framingham, MA). This material was extensively dialyzed against de-ionized water for two days. Samples of melanin in H_2O, at a concentration of 40 mg/ml and adjusted to pH 8 with sodium hydroxide, were prepared without copper and with different concentrations of copper ions. In order to estimate a molecular weight for the melanin samples, we assumed a protomolecule consisting of ~6 indolequinone units per layer and with ~3 layers yielding an initial melanin molecular weight estimate of 3000. Thus, at a concentration of 40 mg/ml, the concentration of melanin, in moles per liter, was 0.013. The copper ions were added to the solution in the form of copper sulfate, giving copper ion-to-melanin molar ratios ranging from 0.01 to 1.0. All melanin solutions containing copper ions were allowed to incubate for 24 h to ensure that equilibrium conditions were achieved.

Small-angle scattering

SANS experiments were carried out at the small-angle diffractometer (SAD) (Thiyagarajan et al., 1997) at Argonne's Intense Pulsed Neutron Source. SAD uses pulsed neutrons with wavelengths in the range of 0.5–14 Å and a fixed sample-to-detector distance of 1.54 meters. The scattered neutrons are measured using a 64×64 array 20×20 cm^2 in area of position-sensitive, gas-filled proportional counters while their wavelengths are selected by time-of-flight by binning each neutron pulse into 67 time channels with constant $\Delta t/t = 0.05$. This instrument thus can provide useful SANS data in the Q range of 0.005–0.25 Å^{-1} in a single measurement, where Q is related to the neutron wavelength λ and the scattering angle 2Θ by the expression $Q = 4\pi \sin \Theta/\lambda$. The melanin solutions in D_2O were measured in cylindrical Suprasil cells with a path length of 2 mm, and those in H_2O were measured in cells with a path length of 1 mm. The data for each sample is corrected for the backgrounds from the instrument, the Suprasil cell, and the solvent, as well as for detector nonlinearity. Data are presented on an absolute scale obtained by using the known scattering cross-section of a silica gel sample standard.

Since the SANS data for the samples containing low concentrations of copper ions were statistically unsatisfactory, these samples were studied by SAXS at the BESSRC-CAT beamline at the Advanced Photon Source at the Argonne National Laboratory. The BESSRC-CAT SAXS apparatus was operated with a sample to detector distance of 0.67 meter, using monochromatic synchrotron x-rays with photon energy 8.8 keV corresponding to the x-ray wavelength 1.4 Å. The scattered x-ray intensity distribution was measured using a position-sensitive, gas-filled proportional counter array 20 cm × 20 cm in area consisting of 512 × 512 pixels. In this configuration, the instrument provided useful SAXS data in the Q range of 0.04–0.5 Å^{-1}. The samples were measured in cylindrical quartz

capillary tubes with an inside diameter of 1 mm. The data for each sample are corrected by normalization to the transmitted beam intensity and subtraction of the normalized data from a distilled water sample. These data are all presented on the same arbitrary intensity scale.

RESULTS

The SANS data used in the data analysis are shown in Fig. 1. At the highest copper-to-melanin ratios studied, 0.6 and 1.0, the strong SANS signal at low Q is an indication that, at these concentrations, melanin has already aggregated to form large, extended structures. The data shown for the samples with lower copper-to-melanin ratios are statistically unsatisfactory. The statistical quality of the data measured by SAXS, even at low copper-to-melanin ratios, was far superior, as can be seen from Fig. 2.

It is possible to use SANS data measured with samples of melanin in both H_2O and D_2O to experimentally extract the scattering length density of melanin and compare that with the expected scattering length density based on the chemical formula and density given above. This can be accomplished by utilizing the dependence of the scattering intensity on the scattering length density difference as per Eq. 3. This is done by normalizing the data for melanin concentration in the samples and calculating the scattering length density for melanin, which will cause the two data sets to be superimposed when normalized for the square of the scattering length differences between the melanin and the solvents. On comparison, we find that for the SANS data for samples with a copper-to-melanin ratio of 1.0, shown in Fig. 3, the shape of the scattering curve from samples prepared in both H_2O and D_2O is identical, exhibiting a power law dependence of the form $I(Q) \propto Q^{-2}$. The value for the scattering length density for melanin in D_2O obtained as described above from these data is 5.0×10^{10} cm^{-2}, in good agreement with that calculated from the molecular formula assuming 10 of the melanin protons are replaced with deuterons. Based on this agreement the scattering length density of melanin is 3.58×10^{10} cm^{-2}, and we will use this value for ρ_p in Eqs. 3, 5, and 7 to determine the molecular weight from the SANS data that are on an absolute intensity scale.

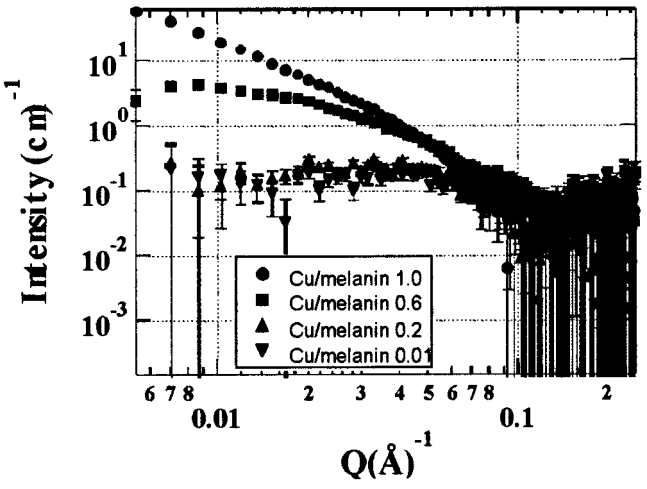

FIGURE 1 Plot of the SANS data for samples of tyrosine melanin used in the analysis. The slopes of the curves for the two more-concentrated samples indicate that these samples have formed large aggregates.

We obtain information on particle size by analyzing the scattering intensity $I(Q)$ in the low Q regime using the Guinier approximation (Guinier and Fournet, 1955),

$$I(Q) = I(0)\exp(-Q^2R_g^2/3), \tag{2}$$

where

$$I(0) = \frac{M_w C(\rho_p - \rho_s)^2}{1000\, N_A d^2}. \tag{3}$$

In Eq. 3, $I(0)$ is the extrapolated intensity at $Q = 0$, ρ_s and ρ_p are the scattering length densities of the solvent and particle, respectively, and C is the concentration of melanin in mg/ml. Equation 2 is used to determine the radius of gyration, R_g, from the slope of a line of a plot of $\ln(I(Q))$ versus Q^2 in the region of Q where $Q_{max}R_g \approx 1$. The value obtained for R_g is the root-mean-squared distances of all the atoms from the centroid of the scattering volume of the particle. The weight-average molecular weight of the aggregates is determined from the y-intercept of this line using Eq. 3. This method was used to obtain values for R_g of 21 ± 3 Å and 21 ± 4 Å for samples of melanin in H_2O with copper-to-melanin ratios of 0.2 and 0.01, respectively. The corresponding values for $I(0)$ are 0.30 ± 0.03 cm^{-1} and 0.24 ± 0.03 cm^{-1}, leading to values for the molecular weight of 52 ± 5 and 41 ± 5. The SANS data for the other samples with low copper concentrations were of insufficient quality for reliable Guinier analysis, and the samples with copper-to-melanin ratios of 0.6 and 1.0 formed aggregates that are too large for Guinier analysis of the data to be used to determine values for R_g.

Guinier analysis of the SAXS data measured for the melanin samples with copper-to-melanin ratios of 0, 0.1, and 0.2 yielded R_g values of 18.40 ± 0.29 Å, 19.29 ± 0.42 Å, and 19.88 ± 0.31 Å, respectively. The quality of the Guinier analyses of data measured by SANS and SAXS for the sample with a copper-to-melanin ratio of 0.2 is compared in Fig. 4. Since the absolute intensity scale of the SAXS data has not been calibrated we can derive only the structure of the aggregates, but not their molecular weight.

If a particle is sheet-like or, in other words, is much smaller in one dimension than the other two, then the average thickness T of the particle can be measured using the modified Guinier approximation for sheet-like forms (Porod, 1982):

$$I(Q) = Q^{-2}I_T\exp(-Q^2T^2/12), \tag{4}$$

where

$$I_T(0) = \frac{2\pi M_w C(\rho_p - \rho_s)^2}{1000\, N_A d^2 A}. \tag{5}$$

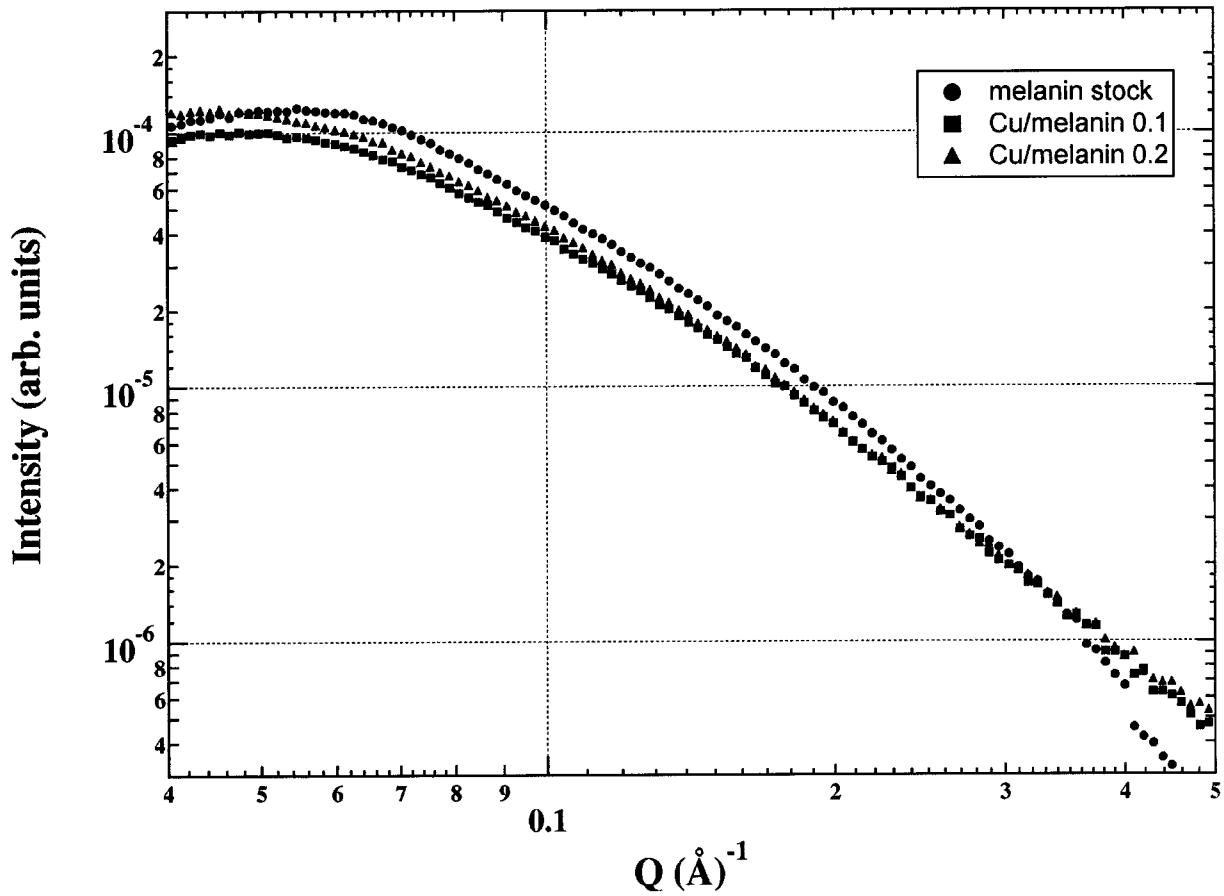

FIGURE 2 Plot of the SAXS data for samples of tyrosine melanin with low copper ion-to-melanin ratios. The higher intensity and more pronounced curvature at low Q of the sample without copper is due to concentration of the sample by evaporation during storage. Note the much-improved statistical quality of the data.

In Eq. 5, A is the area of the particle in Å^2. Equation 4 is used to determine the thickness T from the slope of the line on a plot of $\ln(Q^2I(Q))$ versus Q^2 in the region of Q where $Q_{max}T \approx \sqrt{12}$. The plot used for the modified Guinier analysis for sheet-like forms of the SAXS data for the sample with a copper-to-melanin ratio of 0.2 is illustrated in Fig. 5. When this method is used to analyze the SAXS data for the samples with copper-to-melanin ratios of 0.0, 0.1, and 0.2, we find that the melanin in these samples is present in the form of small lamellar particles. The average thicknesses of these particles are 12.89 ± 0.08 Å, 11.90 ± 0.11 Å, and 12.82 ± 0.10 Å, respectively.

Modified Guinier analysis for sheet-like forms of the SANS data for the sample with a copper-to-melanin ratio of 1.0, shown in Fig. 6, demonstrates that the melanin aggregates at this copper concentration are also sheet-like in form. These aggregates have an average thickness of 51.0 ± 1.3 Å. Since the SANS data are measured on an absolute scale, the average molecular weight per unit area of these particles is calculated from the y-intercept of this plot using Eq. 5 to be 64 ± 7. Similar analysis of the SANS data for the sample with a copper-to-melanin ratio of 0.6 shows that the melanin aggregates in this sample are not sheet-like, but rod-like, as discussed below.

To understand the structure of the large melanin aggregates in the sample with a copper-to-melanin ratio of 0.6, we analyzed the SANS data for this sample using modified Guinier analysis for rod-like forms (Porod, 1982). In this type of analysis, the scattered intensity in the low Q region is approximated by the equation

$$I(Q) = I_C(0)\exp(-Q^2R_C^2/2), \tag{6}$$

where

$$I_C(0) = \frac{\pi M_w C(\rho_p - \rho_s)^2}{1000\, N_A d^2 L}. \tag{7}$$

In Eq. 7, L is the length of the rod-like aggregate. Equation 6 is used to determine the cross-sectional radius of gyration, R_C, from the slope of the line on Fig. 7, a plot of $\ln(QI(Q))$ versus Q^2, in the region of Q where $Q_{max}R_C \approx 1$. The value obtained for R_C is the root-mean-square of the distances of all of the atoms in a cross-section of the rod to the centroid of this cross-section. Equation 7 is used to determine the molecular weight per unit length along the axis of the aggregate from the y-intercept. This analysis yields a value for R_C of 23.2 ± 0.9 Å (radius = 32.8 ± 1.3 Å) and an average molecular weight per unit length of 2.77 ± 0.28.

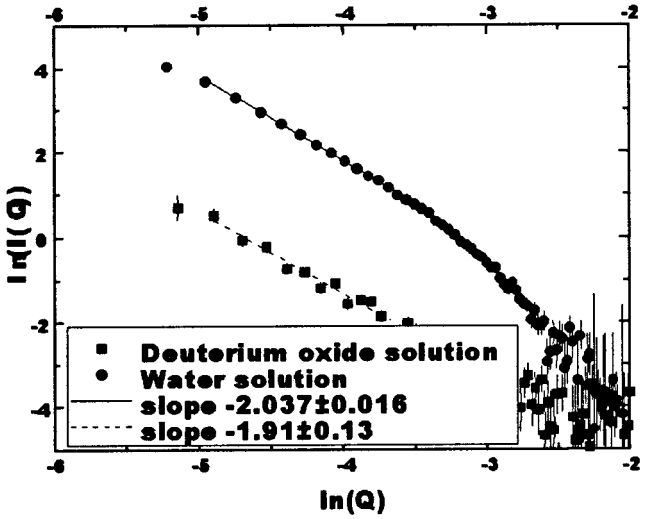

FIGURE 3 Comparison of the power-law scattering measured for the samples with a copper-to-melanin ratio prepared in H_2O and D_2O. Note the similar shapes of the two curves and much higher intensity of the H_2O data. The observed power-law dependence is consistent with the scattering from either a sheet-like object or a mass fractal with dimension 2.

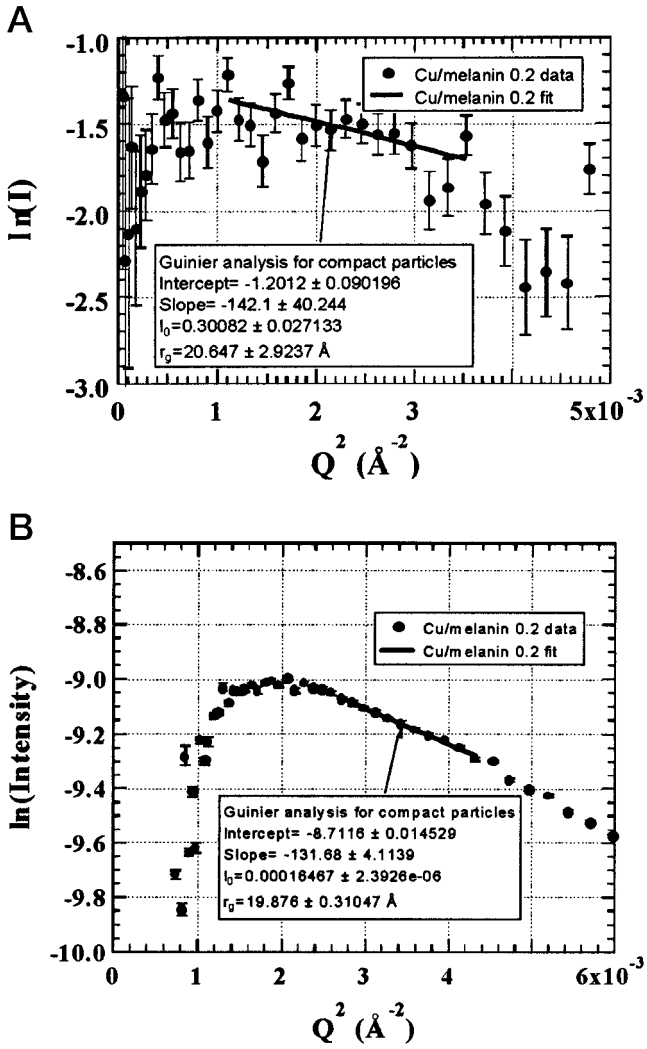

FIGURE 4 Comparison of the Guinier plots of the data for the sample with a copper-to-melanin ratio of 0.2 measured using (*A*) SANS and (*B*) SAXS. The large statistical fluctuations in the SANS data are a result of subtraction of the large background scattering due to water.

DISCUSSION

Our objectives in this work were to place an upper limit on the minimum size of melanin molecules or aggregates in well-dispersed aqueous solutions and to investigate the size and morphology of melanin aggregates formed in the presence of copper ions.

According to our recent STM study (Zajac et al., 1994) the fundamental or unaggregated melanin is nominally 15–20 Å in lateral extent and ~10–12 Å in height, consistent with the model developed from WAXS (Cheng et al., 1994). In this model, approximately six monomers of 5,6-dihydroxyindolequinone (mol wt ~0.15) are assumed to form a planar structure, yielding a molecular weight per layer of 0.9. The protomolecule of melanin consists of three to four such layers, corresponding to a molecular weight of 3.5.

The present SAXS study of melanin solutions with low copper-to-melanin ratios shows that the particles have an R_g ~18 Å. Since the R_g of the protomolecule is ~7 Å the melanin solution should contain aggregates of these molecules. To further understand how the association occurs we performed modified Guinier analysis for sheet-like form of the SAXS data that gave an average thickness of 12.5 Å. This value is very close to the height of the melanin protomolecule with 3 or 4 layers (10.2 Å and 13.6 Å, respectively) described above. This nearly constant particle thickness suggests that the particles in melanin solutions exist as aggregates of melanin protomolecules joined edgewise in the lateral direction. This, together with the fact that R_g and the molecular weight of the particles increase with increasing copper-to-melanin ratio, implies that the growth of these, due to the presence of copper ions, initially occurs by the addition of the fundamental molecular stacks at their edges. If we assume that the melanin particles are shaped like thin circular disks, then the radius of these disks can be determined from the thickness and R_g by using the expression

$$r = \sqrt{2(R_g^2 + T^2/12)}. \quad (8)$$

Thus, the SAXS data measured for the melanin samples with copper-to-melanin ratios of 0, 0.1, and 0.2 suggest that they are in the form of disk-like particles with radii of 25.4 Å, 26.8 Å, and 27.6 Å, respectively. This size corresponds to an aggregation number of 9 to 11 protomolecules, assuming that the area of one protomolecule is 225 Å^2. Similarly, the radius of the particles derived from the SANS data for the samples with copper-to-melanin ratios of 0.01 and 0.2 is 29 ± 5 Å, corresponding in area to 12 ± 4 protomolecules. Interestingly, this is in very good agreement with the aggregation number of 12 to 15 protomol-

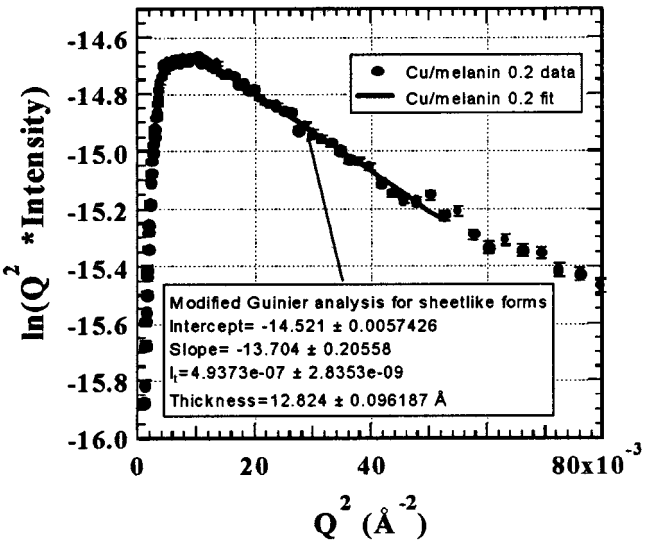

FIGURE 5 An example of the modified Guinier plots for sheet-like forms of the SAXS data for the samples with low copper ion concentrations. The excellent agreement between the data and the fitted line indicates that the melanin particles in these samples are indeed lamellar in form.

ecules derived from the molecular weights obtained from our SANS data for these same samples.

At copper-to-melanin of 0.6 the scattering intensity profile shows that the melanin aggregates are now in the form of extended, rod-like structures. Since the radius of a cylinder is related to R_C by the expression

$$r = \sqrt{2}R_C, \tag{9}$$

the measured R_C value of 23.2 ± 0.9 Å for this sample leads to a cylinder radius of 32.8 ± 1.3 Å. This would correspond in area to ~15 of the melanin particles observed by STM.

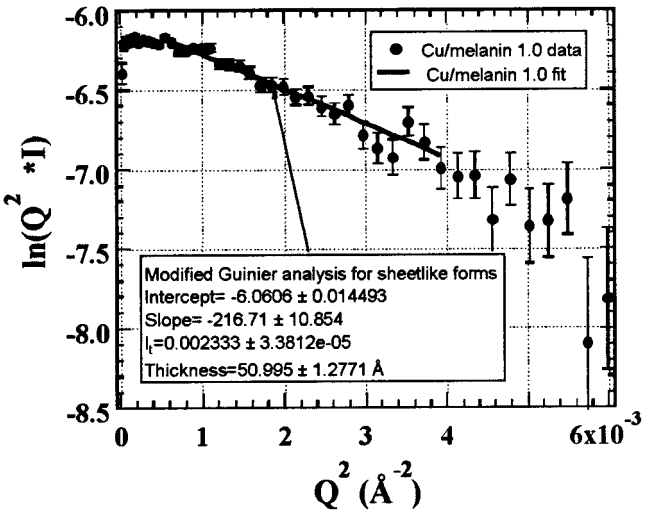

FIGURE 6 Modified Guinier plot for sheet-like forms of the SANS data for the sample with a copper-to-melanin ratio of 1.0. This analysis shows that high concentrations of copper ions cause melanin to aggregate into thick sheets.

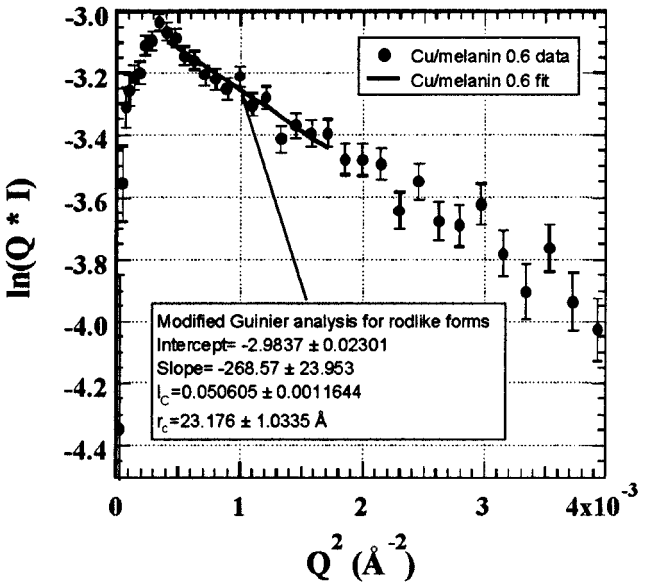

FIGURE 7 Modified Guinier plot for rod-like forms of the SANS data for the sample with a copper-to-melanin ratio of 0.6. The average radius of the rod-like melanin aggregates as measured by this analysis is compatible with both the radii of the lamellar particles observed at lower copper concentrations and the thickness of the sheet-like aggregates observed at higher concentrations.

Therefore, these rod-like aggregates would appear to consist of stacks of lamellar aggregates of ~15 of these melanin protomolecules. However, the calculated mass per unit length of these rods leads to a molecular weight of 35 ± 4 for a section 12.5 Å in length, 33% lower than the value expected for 15 melanin stacks. Since the experimentally determined mass is an average value weighted by the number and the mass squared of each kind of particle in the solution, this discrepancy is probably due to the presence of melanin in the sample in other, less aggregated states.

The rod-like aggregates observed at intermediate copper concentrations would naturally lead to more complicated structures at the higher copper ion concentrations. The power-law behavior exhibited by the SANS data of melanin solutions with a copper-to-melanin ratio of 1.0 with respect to Q is consistent with the scattering from either an extended sheet-like structure or a mass fractal with a dimension of 2. The previous light-scattering study on melanin in solution at low pH attributed the scattering to be due to fractal objects (Huang et al., 1989). We believe that the large aggregates are sheet-like rather than fractal objects. The rods seen at a copper-to-melanin ratio of 0.6 appear to further aggregate into sheets in a structure similar to a log raft. Since the average cross-sectional thickness of a rod is related to its radius by the equation

$$T = \pi r/2, \tag{10}$$

the observed thickness of these sheets, 51.0 ± 1.3 Å, is consistent with a sheet of rod-like units with a radius of 32.5 ± 0.8 Å. Thus, this calculated radius is in excellent

agreement with the value for the radius of the rod-like aggregates calculated from the data for the sample with a copper-to-melanin ratio of 0.6. The results of this analysis are consistent with the view that the sheet is composed of disk-like lamellar particles of ~15 melanin protomolecules viewed edgewise or, more likely, rod-like aggregates of these particles viewed perpendicular to their longitudinal axes. The measured mass per unit area of sample gives a mass of 52 ± 5 kD for an area of the sheet that is 12.5 Å by 65 Å, in agreement with the size information.

Our results for melanin at normal pH values (7–8) and free of metal ions are in relatively good agreement with previous measurements using SAXS methods (e.g., Miyake et al., 1986; Cheng et al., 1994), where R_g values ranged between ~15 and ~50 Å. However, our results differ significantly from the R_g values obtained by visible light-scattering methods (Bridelli, 1998). There are several possible explanations for the differences between these SAXS and visible light-scattering results. One reason may be related to any differences in the polymerization techniques used to make the samples. Another reason may relate to the inherent limitations of the scattering techniques used. By using small-angle scattering techniques we are able to extract shape, size, and molecular weight information with a much higher resolution than is possible at these short length scales by visible light-scattering methods. However, we are unable to probe information on the much longer-length scales corresponding to the overall size of heavily aggregated melanin particles. In contrast, the light-scattering experiment studied the dynamics of assembly and the global size and structure of large-scale melanin aggregates, not the local structure of their fundamental building blocks.

Although the measured "fractal" dimension of our most aggregated sample, the sample with a copper-to-melanin ratio of 1, is in agreement with the fractal dimensions of highly aggregated melanin structures obtained by light-scattering techniques, the excellent agreement of the fit for the modified Guinier function for sheet-like forms with the data indicates that the melanin structures in this sample are sheet-like instead of fractal in form. In particular, the agreement between the molecular weight calculated for this sample and the samples at low copper concentrations indicates that the melanin structures in the sample with the highest copper-to-melanin ratio are also compact. The much lower molecular weights per unit volume measured for the large-scale aggregates indicates that these are less dense, more open structures, perhaps formed by the branching and intertwining of the sheet- and rod-like structures that we have observed.

The observation that either the addition of metal ions to or acidification of aqueous melanin solutions both lead to large aggregates of melanin deserves further comment. At sufficiently high pH, melanin is highly dispersed in aqueous media and shows little scattering of visible light. When the pH is lowered, aggregation is easily observed for tyrosine or L-dopa melanin, and significant aggregation begins to occur at a pH value of 4. The suspension stability of melanin in water is most likely related to the presence of the various ionizable groups in its structure. Although their types and ratios may vary depending upon the particular melanin precursor, these groups generally consist of a mixture of phenol, amine, and carboxyl units, each having their own pK values. For tyrosine-derived melanin, all of these units are present. At high pH, these groups are ionized as the structures COO^- and OH^-. As the pH is lowered, excess H^+ ions protonate the ionizable groups and the suspension stability is destroyed and aggregation begins. This view is in accord with recent light-scattering results and analysis for both natural and synthetic melanins (Bridelli, 1998).

Metal ions such as Cu^{2+} can also induce an effect similar to acidification. At sufficiently high concentration most divalent metal ions will induce aggregation in aqueous solutions of melanin. Furthermore, melanin has a strong affinity for divalent metal ions, forming ligands and chelates more aggressively than EDTA (Sarna et al., 1980). In this regard, metal ions will behave differently from acidification, so that in addition to inducing aggregation by protonating the ionizable groups, they will also produce complexes among the fundamental melanin protomolecules. Although van der Waal forces are likely to influence the stacking and aggregation of melanin, our present data support a model for the copper-induced aggregation of melanin driven primarily by π stacking assisted by peripheral Cu^{2+} complexation. Molecular modeling is currently underway in our group to characterize the possible bimolecular structures of tyrosine melanin molecules chelated by copper ions.

As of now, the details of the synthesis of natural melanin within the surrounding protein matrix of the melanocyte are still unknown. However, given that the 3.4 Å repeat distance shows up in the diffraction data for some natural eumelanins (Cheng et al., 1994) and the fact that the synthetic melanins have been generally good models for the natural melanins, it is likely that the protomolecule model is also valid for naturally occurring melanin. It is from this point that metal ion-induced aggregation, of the type described in this paper, could proceed, possibly constrained by the protein structure. SANS experiments to study the structure in solution of both synthetic and natural melanins associated with proteins are underway.

Finally, with regard to the biological implications for cellular protection by melanin-copper aggregates, the present structural studies may be relevant to a recent hypothesis (Sarna, 1992) that attempts to explain one basis for melanin protection: in the case of RPE melanin, oxidative damage to cells could occur from oxidizing species that result from the interaction of redox-active metal ions (such as copper) with hydrogen peroxide. If such interactions occur while the metal ions are bound to the melanin polymer, subsequent reactions with the oxidizing species will be limited by their diffusion-controlled reactions with reaction centers within the melanin aggregate. It is reasonable to expect that the character of such reactions will be influenced by the specific structures of the melanin-metal ion aggregates.

SUMMARY

SANS and SAXS techniques are used to observe the formation of small aggregates of melanin induced by the addition of copper ions. Guinier and modified Guinier analyses of small-angle scattering data for the samples containing copper ions indicate that melanin forms lamellar aggregates with a thickness of ~12.5 Å at low copper concentrations. At higher copper concentrations, these lamellar particles stack to form larger, rod-like aggregates with a radius of 33 Å. When the copper-to-melanin ratio is increased further, these rod-like structures form sheets with a thickness of 51 Å, apparently by aligning with their axes parallel. This complicated, concentration-dependent metal ion-induced aggregation of melanin in solution observed by SANS and SAXS is consistent with the known influence of metal ions to cause aggregation of melanin and is a natural consequence of the π stacked molecular systems.

NOTES

1. If the dimensions of the melanin protomolecule are assumed to be 15–20 Å in lateral extent and ~10 Å in height, then this result follows from the geometrical formula relating the radius of gyration R_g to the sides of a prism, $R_g^2 = [A^2 + B^2 + C^2]/12$ (Glater, 1982).

2. It is well-understood that melanin is a heterogeneous polyphenol existing simultaneously in both oxidized and reduced forms by incorporating the various oxidation-reduction intermediates that occur subsequent to the initial oxidation of the precursor. It thus includes, in addition to the metal-chelating phenols, carboxyl and amine groups, which can form ligands with a variety of divalent metal ions. The simple homogeneous model of 5,6-indolequinone used in the x-ray model is not sensitive to the changes that occur by adding the complexity of such groups.

We gratefully acknowledge the technical support provided by D. G. Wozniak at IPNS.

This work benefited from the use of a SANS instrument at IPNS and a SAXS instrument at BESSRC-CAT at APS, which are supported by the U.S. Department of Energy Office of Basic Energy Sciences Division of Material Sciences under Contract W-31-109-Eng-38 to the University of Chicago.

REFERENCES

Bridelli, M. G. 1998. Self-assembly of melanin studied by laser light scattering. *Biophys. Chem.* 73:227–239.

Chedekel, M. R. 1995. Photophysics and photochemistry of melanin. *In* Melanin: Its Role in Human Photoprotection. L. Zeise, M. R. Chedekel, and T. B. Fitzpatrick, editors. Valdenmar Publishing Co., Overland Park, KS.

Cheng, J., S. C. Moss, M. Eisner, and P. Zschack. 1994. X-ray characterization of melanins. I. *Pigment Cell Res.* 7:255–262.

Chio, S. S. 1977. X-ray diffraction and ESR studies on amorphous melanin. Ph.D. Thesis, University of Houston.

Eisner, M. 1992. The physical and chemical properties of eye melanin and their relationship to photoprotection. *In* Occhio e Radiazoni Solari, Tecnologie Fotoprotettive e Funzione Visiva. M. Cordella, editor. Universita degli Studi di Parma, Parma, Italy. 61–73.

Glater, G. 1982. Data treatment. *In* Small Angle X-ray Scattering. O. Glatter and O. Kratky, editors. Academic Press, London. 119–165.

Guinier, A., and G. Fournet. 1955. Small Angle Scattering of X-rays. John Wiley and Sons, New York.

Huang, J. S., J. Sung, M. Eisner, S. C. Moss, and J. M. Gallas. 1989. The fractal structure and the dynamics of aggregation of synthetic melanin in low pH aqueous solutions. *J. Chem. Phys.* 90:25–29.

Ishii, T. 1984. Melanin in the human inner ear. *In* Structure and Function of Melanin. 1. K. Jimbow, editor. Fuji, Ltd., Sapporo, Japan. 43–48.

Kollias, N. 1995. Melanin and non-melanin photoprotection. *In* Melanin: Its Role in Human Photoprotection. L. Zeise, M. R. Chedekel, and T. B. Fitzpatrick, editors. Valdenmar Publishing Co., Overland Park, KS. 233–238.

Kozikowski, S. D., L. J. Wolfram, and R. R. Alfano, 1984. Fluorescence spectroscopy of melanins. *IEEE J. Quant. Elec.* QE-20:1379–1382.

Miyake, Y., Y. Izumi, A. Tsutsumi, and K. Jimbow. 1986. Chemicophysical properties of melanin III. *In* Structure and Function of Melanin 3. K. Jimbow, editor. Fuji, Ltd., Sapporo, Japan. 3–18.

Pathak, M. A., and T. Fitzpatrick. 1974. The role of natural photoprotective agents in human skin. *In* Sunlight and Man. M. A. Pathak, L. C. Harber, M. Seiji, A. Kukita, and T. B. Fitzpatrick, editors. Univ. of Tokyo Press, Tokyo. 725–750.

Porod, G. 1982. General theory. *In* Small Angle X-ray Scattering. O. Glatter and O. Kratky, editors. Academic Press, London. 17–51.

Sarna, T. 1992. Properties and function of the ocular melanin: a photobiophysical view. *J. Photochem. Photobiol., B. Biol.* 12:215–258.

Sarna, T., W. Froncisz, and J. S. Hyde. 1980. Cu^{2+} probe of metal-ion binding sites in melanin using electron paramagnetic resonance spectroscopy. II. Natural melanin. *Arch. Biochem. Biophys.* 202:304–313.

Thiyagarajan, P., J. E. Epperson, R. K. Crawford, J. M. Carpenter, T. E. Klippert, and D. G. Wozniak. 1997. The time-of-flight small angle neutron diffractometer (SAD) at IPNS, Argonne National Laboratory. *J. Appl. Crystallogr.* 30:280–293.

Young, W. Y. 1988. Solar radiation and age-related macular degeneration. *Survey of Ophthalmology.* 32:252–269.

Zajac, G. W., J. M. Gallas, J. Cheng, M. Eisner, and S. C. Moss. 1994. The fundamental unit of melanin: a verification by tunneling microscopy of x-ray scattering results. *Biochim. Biophys. Acta.* 1199:271–278.

Zeise, L. 1995. Analytical methods for characterization and identification of eumelanins. *In* Melanin: Its Role in Human Photoprotection. L. Zeise, M. R. Chedekel, and T. B. Fitzpatrick, editors. Valdenmar Publishing Co., Overland Park, KS. 11–22.